Chapter 1

Introduction

1.1 Motivation

International Energy Outlook 2021 of the Energy Information Administration (EIA) projects that global energy consumption and carbon dioxide emissions will increase nearly by 50% by 2050 due to population and economic growth. According to the latest edition of the IEA's semi-annual Electricity Market Report, after falling by about 1% in 2020 due to the effects of the Covid-19 pandemic, global electricity demand is expected to grow by close 5% in 2021 and 4% in 2022. According to the latest edition of the IEA's semi-annual Electricity Market Report released. The Asia Pacific area, particularly China and India, is predicted to account for the majority of the rise in power consumption.

Figure 1.1 presents the projection of the energy consumption in British thermal units(BTU: 1 BTU=1055.05585 Joule). It can be observed from the projected data that the global energy demand is set to increase by around 50 % by 2050. At the same time, the percentage share of renewable energy in the global energy supply is set to increase as well. Renewable capacity additions increased by more than 46% from 2019 to 2020. An exceptional 192% rise in global wind capacity additions led to the expansion. Also underpinning this record growth was the 25% expansion of new solar PV installations to almost 135 GW [10].

Thus, the renewable energy market has been experiencing rapid growth in recent decade [11]. The solar/photovoltaic (PV) and wind power conversion systems(WECS) are leading this unprecedented growth [12, 13]. The major problem with the PV and WECS is the intermittent nature of availability; thus, a hybrid PV-Wind generation system is

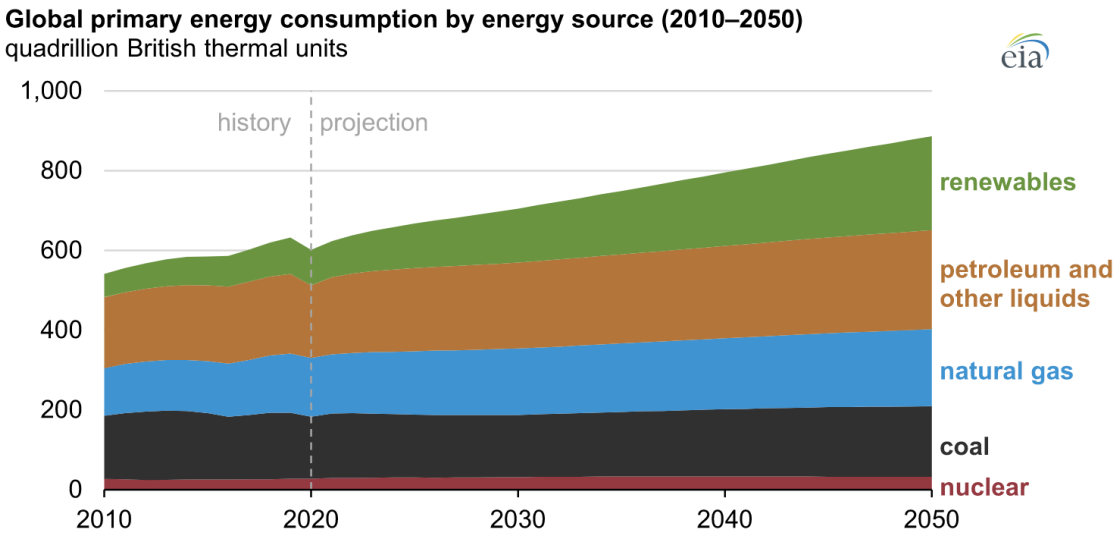

Figure 1.1: Projection of energy consumption based on source type.

put forth [14–17].

Figure 1.2 shows the hourly distribution of the solar and wind power availability. It is evident that the power generation is complementary in nature, and the cogeneration from PV and WECS gives a more stable profile of generation. Apart from the daily distribution, the annual power generation distribution is also found to be complementary in nature, as shown in Figure 1.3. This complementary nature of the PV and WECS makes them the perfect candidate for developing the hybrid power generation system. The PV and WECS have many limitations which motivate this work, and some investigations are carried out in order to find these limitations. Hereby, some solutions are put forth to alleviate these limitations.

The working of the PV generations and WECS are presented henceforth, in order to identify the associated problems with these systems.

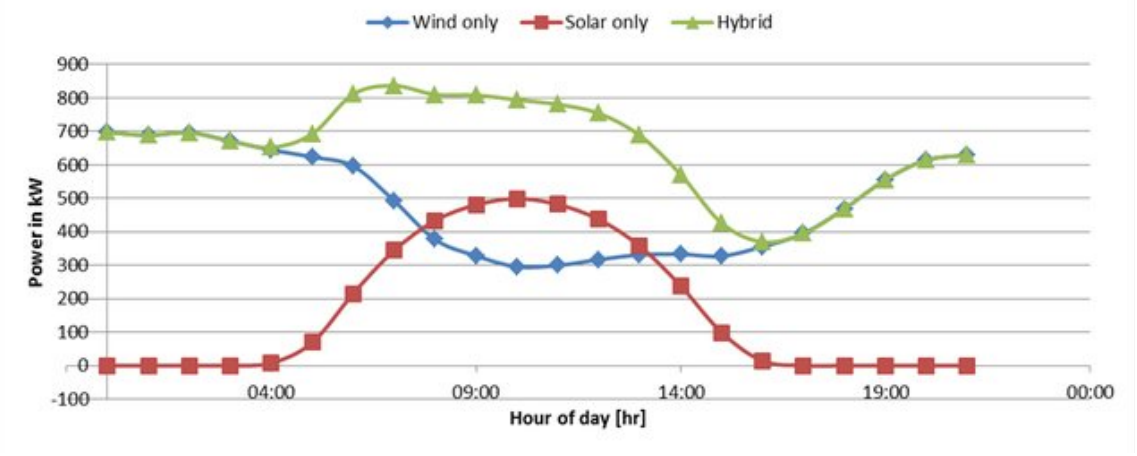

Figure 1.2: Typical daily distribution of solar, wind and hybrid power generation.

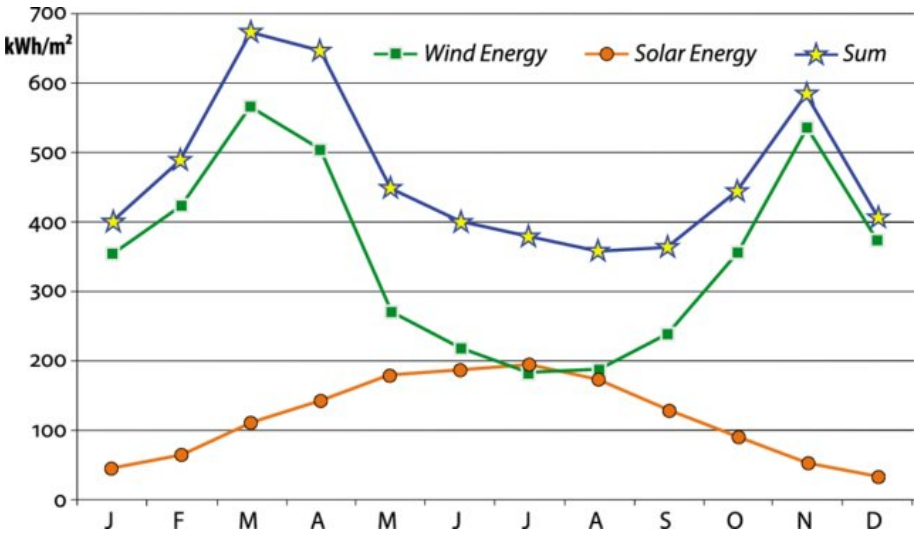

Figure 1.3: Typical annual distribution of solar, wind and hybrid power generation.

1.2 Solar Power Generation

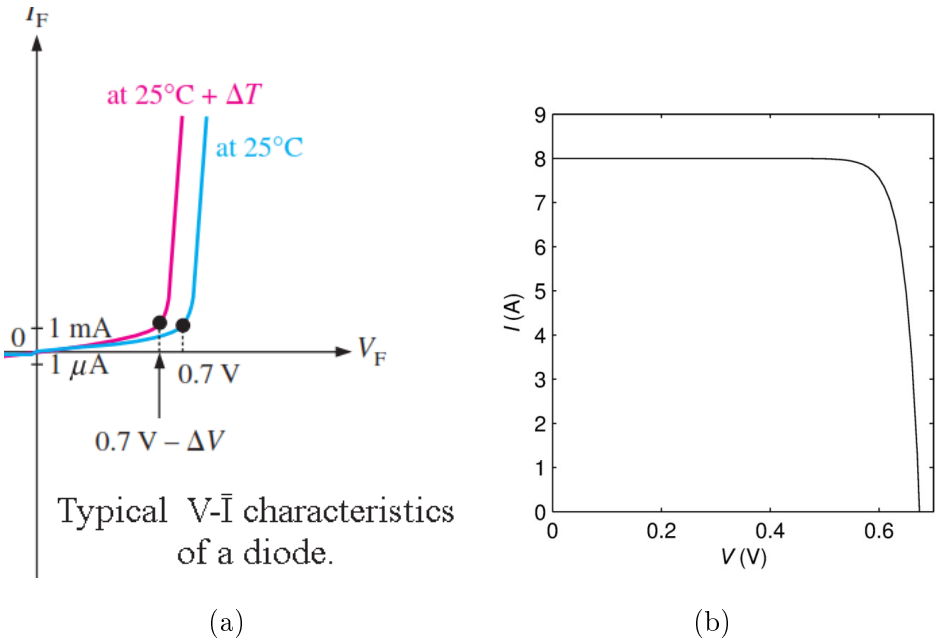

(a) (b)

Figure 1.4: The derivation of the I-V characteristics of PV cell

The typical V-I characteristic of a p-n junction diode is shown in Figure 1.4a, which varies with change in temperature. It can be observed that the forward breakdown voltage of the diode is close to 0.7 V in the case of silicon at room temperature. The PV cell is also a p-n junction diode which is designed to let the light penetrate the junction area in order to develop electron-hole pairs. These generated free charges cause a current to flow across a closed circuit across the diode. This current is called the light current(I_L), which shifts the V-I characteristic of the diode in the fourth quadrant. After taking a mirror image of this shifted V-I characteristic across the voltage axis, the V-I characteristic of a PV cell is generated as shown in Figure 1.4b.

The expression for the V-I characteristic of solar cell is given by [18]:

$$I = I_o \left[exp\left(\frac{qV}{nKT}\right) - 1 \right] - I_L \tag{1.1}$$

The PV cell is inherently a low voltage and high current source, but this problem can be easily solved by using a long string of solar cells in order to get high voltage levels. But developing very high voltage systems using PV cells leads to many problems such as:

- Predominant shading effect, as PV cells with low levels of irradiance starts acting as loads, which leads to heating of PV panels and subsequent efficiency degradation

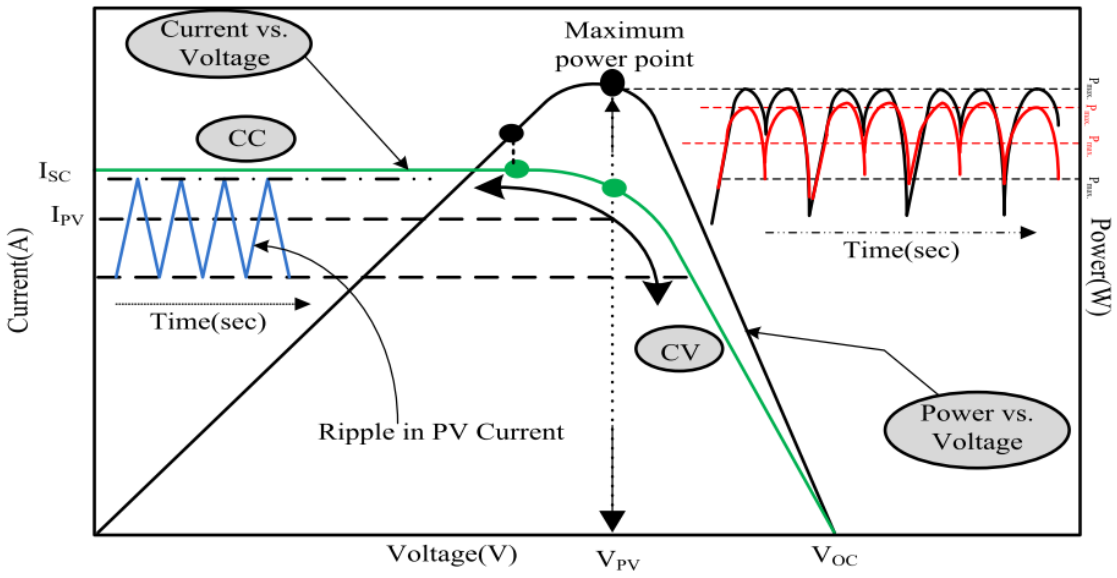

Figure 1.5: MPP oscillation owing to ripple in the output current of the solar panel

[19].

- A small amount of leakage current starts flowing on the surface of the PV panels when PV panels experience a higher level of operating voltages. This small current is responsible for the ionization of the panel glass surface as well as degradation of the p-n junction, and this leads to a reduced operational lifetime of the PV panels. This is called Potential induced degradation(PID) [20].

Another problem associated with the operation of the PV generation system is the oscillation of the maximum power point (MPP). If there is a presence of current ripple in the output of the PV panel, the operating point of the solar panel starts oscillating, which leads to oscillation of the MPP and thus efficiency degradation. It is observed that the presence of only 2.5 % ripple in output current leads to an approximately 7 % fall in PV generation. The oscillation of the MPP is depicted in Figure 1.5

Thus, the problems associated with the PV generation system can be presented as follows:

- The PV generation systems have low output voltage.

- Increasing the output voltage by using long strings leads to potential induced degradation (PID) and predominant shading effect losses.

- Ripple in current from the solar panels oscillates the operating point around the maximum power point (MPP), leading to reduced efficiency and heating of panels.

The possible solutions entail the following:

- A high gain converter to integrate low voltage PV panels with a high voltage DC microgrid. Thus, reducing the problems of predominant shading effect and PID.
- Low-cost DC-DC converter for a highly distributed structure [21].
- Developing a DC-DC converter with low input current ripple to reduce the oscillation of MPP.

1.3 Wind Energy Conversion System

Since the first wind turbine was developed by James Blyth in July of 1887, its innovation and development have been accelerating to the day. Wind turbines from a small battery charger to a ten MW unit are present today. But, for feeding a DC microgrid using distributed generation system, the power level of the wind turbine can only be up to 1-2 kW. The total power that can be extracted from wind at 'v' velocity is given by [22]:

$$Pm = \frac{1}{2} C_p \rho A v^3 \tag{1.2}$$

Where,

$$C_p = C_1(C_2 - C_3 V - C_4 v^x - C_5) e^{-c_6(\lambda,\theta)} \tag{1.3}$$

λ is the tip-speed ratio, i.e., the ratio of the tip speed of the wind turbine and the wind speed. The value of C_p depends on $C_1 - C_6$ and x, and these coefficients are decided by the type of the wind turbine

θ denotes the pitch angle of the wind blades.

ρ is the density of air, its typical value is 1.25 kg/m^3. A is the cross-sectional area of the wind turbine, and V is the wind speed.

The Ideal value of the power coefficient (C_p) is 0.5926. In the field, it is measured to be at the average value of 0.3.

At low power levels and for feeding a DC microgrid, the doubly-fed induction generator(DFIG) can not be used. Thus, a self-excited induction generator (SEIG) and

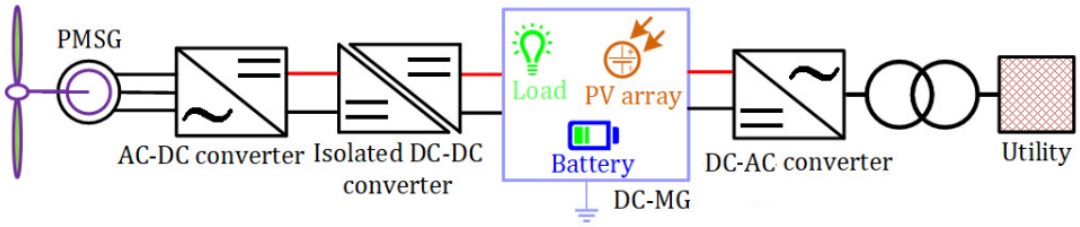

Figure 1.6: Schematic diagram of a PMSG based WECS.

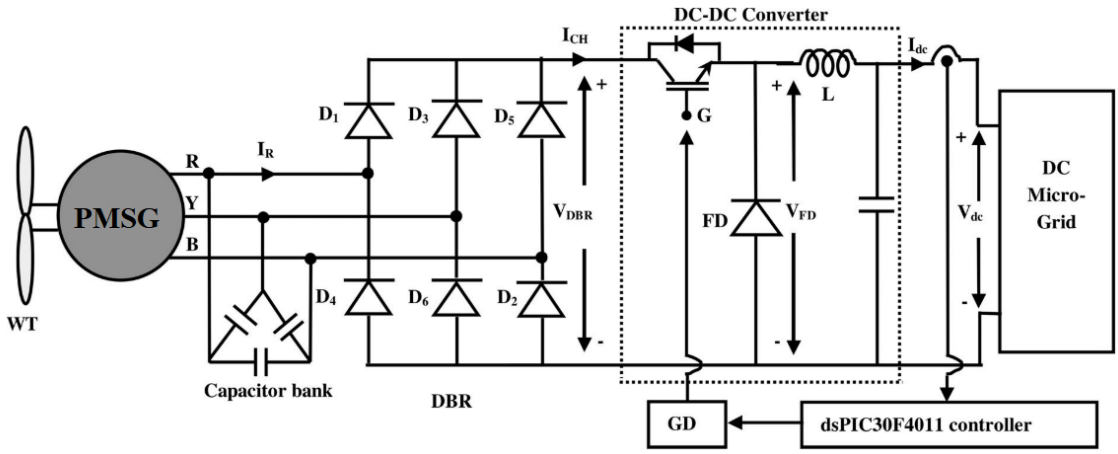

Figure 1.7: Typical WECS with front-end DBR

permanent magnet synchronous generator (PMSG) can only be employed in this system. The SEIG and PMSG based WECS have to use a rectifier for producing DC power from the generated AC power. A schematic diagram representing the two-stage WECS is presented in Figure 1.6. Generally, a diode bridge rectifier (DBR) is used to perform this rectification. The presence of this frontend-DBR reduces the system efficiency by 2-5 %, a typical front-end DBR based WECS is presented in Figure 1.7. Thus a bridgeless converter is developed for single-stage three-phase AC to DC conversion. The developed three-phase converter is operated with both the SEIG and the PMSG based WECS. The problems associated with WECS can be stated as follows [23]:

- Stochastic nature of the wind.
- Requirement of a large area for installation.
- Reduced efficiency due to presence of frond-end diode bridge rectifier(DBR).
- High initial cost of setup for testing.

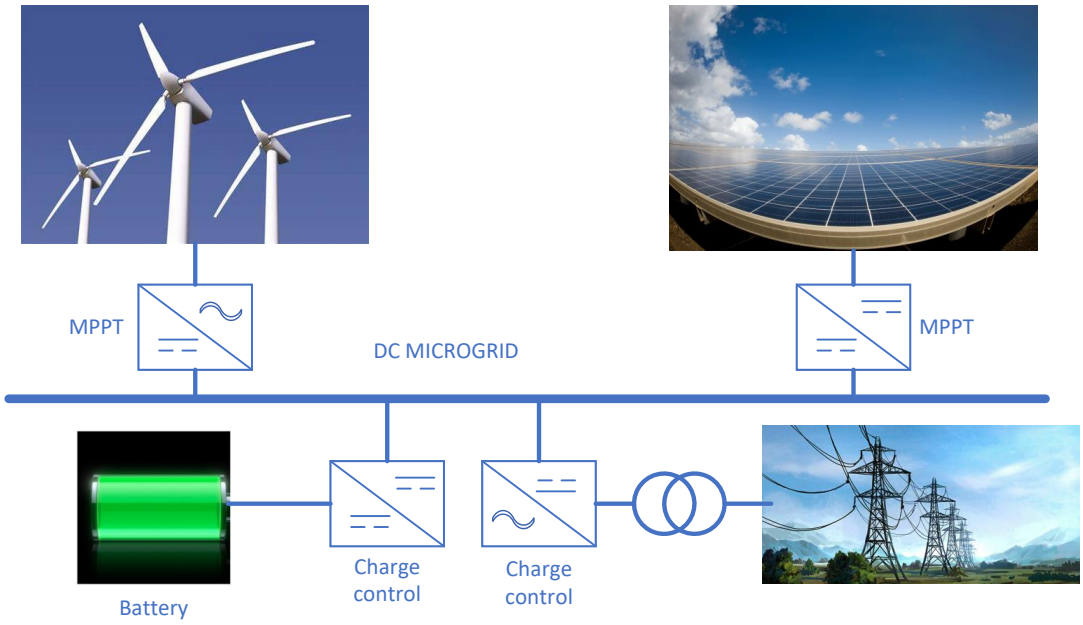

Figure 1.8: The topography of DC microgrid with hybrid sources

To alleviate the above-mentioned problems of the WECS, the following solutions are put forth:

* Development of a wind turbine emulator in the laboratory.

* Development of a bridgeless topology for wind power extraction.

1.4 Hybrid Energy Conversion System

As stated in section 1.1, the solar and wind power generation system are candidates for forming a hybrid energy conversion system HECS. A schematic diagram of a HECS is shown in Figure 1.8, where solar and wind conversion systems are feeding a common DC microgrid. The voltage of the DC microgrid is being regulated using a bidirectional DC-DC converter and a battery energy storage system(BESS) [24, 25]. In this HECS, an alternative method to replace the BESS with the grid is also present [26]. In this work, a methodology to connect the 230 V single-phase grid to the DC microgrid is presented as well [27]. The loss of inertia due to penetration of renewable energy sources makes the BESS-based HECS working In islanded mode preferrable [28–31].

The major focus of this work is to present different power electronic converters for integrating solar, wind, and BESS to the DC microgrid. The converters are developed to address the major limitations of solar and wind power generation systems. A high gain converter with a ripple-free input current is developed to extract the solar power at maximum efficiency and increase the operational lifetime of the solar panels. For WECS, a wind turbine emulator is developed using a PMDC motor and a squirrel cage induction motor (SCIM) as well. Furthermore, a three-phase bridgeless converter is developed to eliminate the front-end DBR. The converter developed for solar power extraction has quadratic gain when operated typically (without input current ripple elimination). Thus, a bidirectional topology of the same converter is designed to integrate the BESS with the DC microgrid.

1.5 Literature Review

1.5.1 Converters for photovoltaic generation systems

There is a vast number of literature available within the last two decades on solar power generation and apt converters for integrating PV generation to a DC microgrid. The development in the control strategies and efficiency of power electronic devices has changed the nature of consumer end loads. Most of the devices process the electric power after changing it in DC form; thus, a DC microgrid is suitable to fulfill the electrification requirement. A detailed study on DC power integration of renewable sources is done in [32], it is observed that the end-to-end efficiency of AC to DC power conversion is only 60 percent compared to 80 percent of DC microgrid to DC loads. Ultra-high gain DC-DC converters using voltage doubler circuits or capacitor-diode cells are presented in [5, 33]. These converters have high voltage gain but have lower efficiency due to the forward voltage drop of diodes carrying high current, and the topology is presented in Figure 1.9. The reduction in the voltage stress is a desirable characteristic of these converters, as it increases the efficiency of conversion and reduction in cost [34].

A high-power high-gain DC-DC converter is presented in [35,36] using Double Active Bridge (DAB) and transformer but has complex control and high component count, which is not suitable for independent modular solar power generation systems. A novel non-isolated DC-DC converter for PV integration with microgrid using a Z-source converter

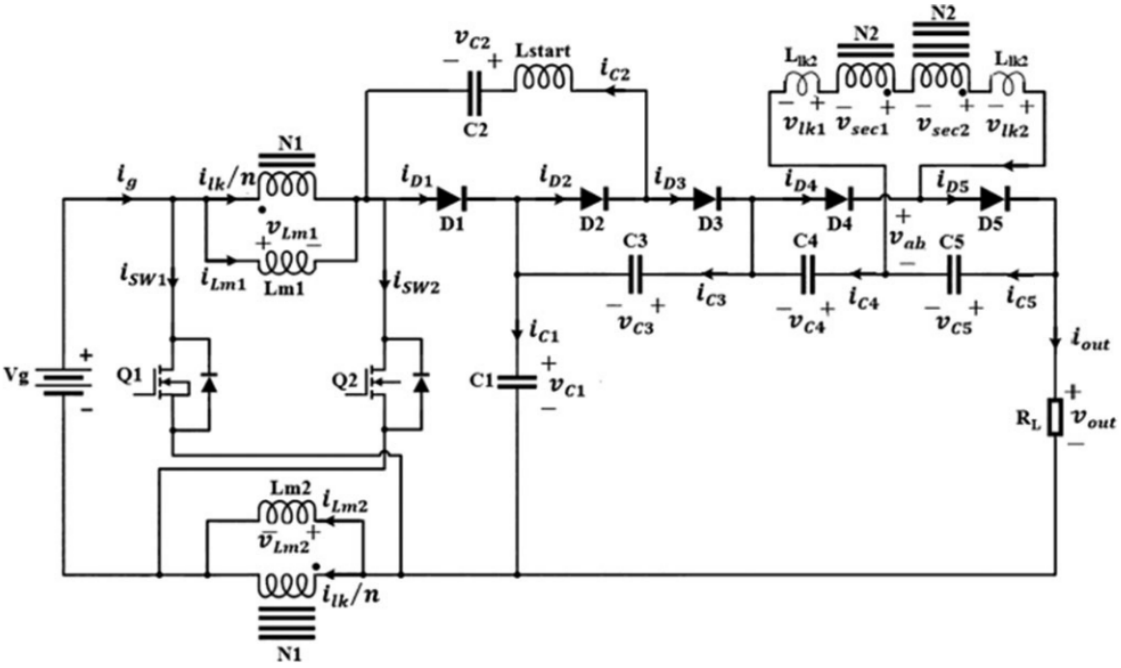

Figure 1.9: Topology of a ultra-high voltage gain converter [5].

with a coupled inductor is proposed in [6] to get high voltage gain. The converter is presented in Figure 1.10; it exhibits high output voltage gain but increased complexity and high component count. A multiport converter with an energy balancing control method is presented in [37], but this converter has a multi-winding transformer requirement leading to a high cost of implementation. [38, 39] presents a versatile converter configuration for EV and grid integration with PV. The presented configuration requires a high voltage PV supply, which is not feasible for a highly distributed PV generation system.

A soft switched interleaved boost converter is presented in [33] for medium voltage grid integration; this converter uses a multi-split output capacitor to achieve high voltage gain. A multi-source interleaved boost converter is proposed in [40] for non-isolated microgrid integration of renewable sources, but the requirement of more than one DC source is not suitable for PV integration as it will not allow MPPT of two or more interleaved PV panel. A high step-up interleaved converter with asymmetric voltage multiplier cell and using coupled inductor is presented in [41–43], but high component count and multiple diodes in series will yield low efficiency at higher output current. The recently presented interleaved converters in [1–4] are shown in Figure 1.11, the converter gain and topological differences are tabulated and compared with the proposed converter in Table 1.1.

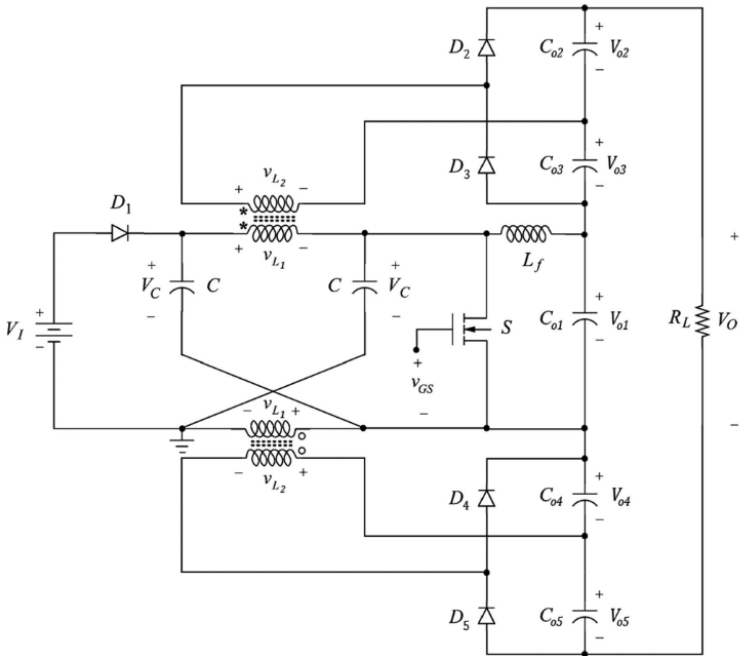

Figure 1.10: Topology of the Z-converter based high gain converter [6]

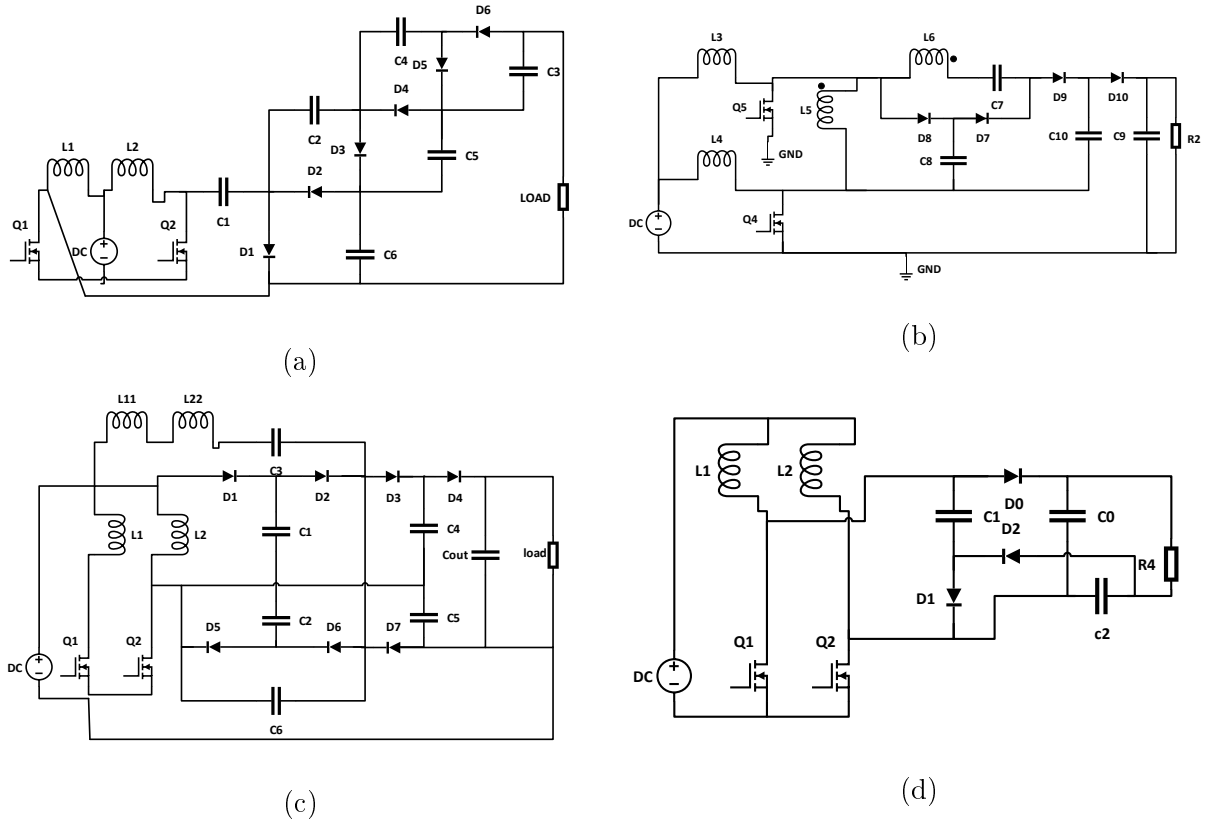

Figure 1.11: Topologies of recently proposed high gain DC-DC converters (a)- [2], (b)- [1], (c)- [3], (d)- [4]

Table 1.1: COMPARISON BETWEEN DIFFERENT INTERLEAVED CONVERTERS

Converter	Number of diodes	Phase increment complexity	Number of capacitors	Output voltage
Interleaved high step-up converter [2]	2	High	4	$\frac{(2N+4)V_i}{1-D}$
Multilevel boost converter [1]	2N	Not possible	2N	$-N\frac{D_1+d_2}{d_2}V_i$
High step-up interleaved with coupled inductor [3]	3N+1	Easy	3N+1	$\frac{8V_i}{1-D}$
High voltage-gain capacitor clamped [4]	2N	High	N+1	$\frac{3V_i}{1-D}$
High gain reduced voltage [104]	2	Easy	2	$V_c + \frac{V_i}{1-D}$

In all the presented modified high gain interleaved boost converter topologies, the per phase component requirement is high, as there is no common component in the interleaved phases.

Directly coupling the photovoltaic (PV) generation system to a DC microgrid using high-gain non-isolated DC-DC converters is an area of immense interest [44–51]. Current ripple reduction is essential with high gain for solar power generation systems. A converter utilizing coupled inductors for ripple-free input current is presented in [52–55]. The power rating of the converter is limited by size constraint, as all the power is being transferred through the coupled inductor. A tri-state interleaved buck-boost converter is presented in [56] with an excellent transient response but has low voltage gain and exhibits ripple-free operation only at a particular duty. An interleaved SEPIC converter with zero-ripple in input-current is presented in [57, 58], using coupled inductors and a clamping circuit. This converter has a high component count and is not suitable for high input current, as interleaving of this converter is not possible with any common components between the phases. In [59, 60], a resonant converter with ripple-free input current is presented using a dual active bridge (DAB) configuration. In this converter, the duty of primary side switches is fixed at 0.5, which eliminates the input current ripple. However, the presence of a transformer between the active bridges deteriorates the overall system efficiency [61]. A

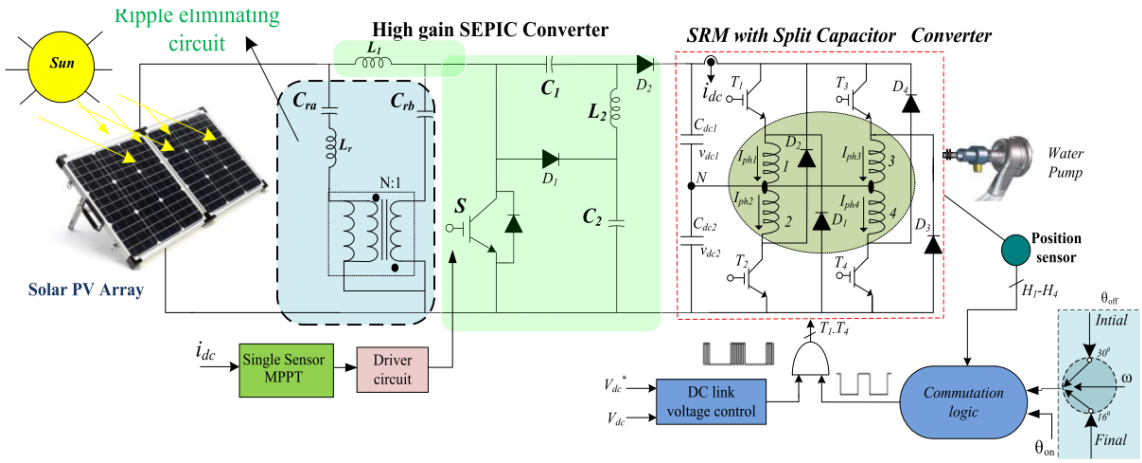

Figure 1.12: Topology of a input-current-ripple elimination converter [7].

ripple elimination circuit is employed in [7] to eliminate the input current ripple, followed by a SEPIC converter. The use of SEPIC topology makes the buck operation of the converter redundant when used in DC microgrids, as the output voltage is clamped at a high value than the input voltage. The converter topology with the current elimination circuit is presented in Figure 1.12.

A semi-quadratic buck-boost converter is presented in [62], a continuous input current is maintained by interleaving the input side. It is evident that the gain of the converter is dependent on the duty of the input-side switches. Thus, the current ripple depends on the voltage gain of the converter. A non-inverting high gain converter is presented in [63], which is a quadratic boost converter-based topology with a voltage doubler circuit. As interleaving with common components between phases is not possible in this topology, moreover the current through the single switch is high. Thus, decreasing the reliability and lowering the efficiency. [64]. [65, 66] presents a quadratic boost converter with a voltage doubler circuit using a high-frequency transformer. Although the current ripple is reduced and has low voltage stress on the switch, this converter topology has a high component count.

1.5.2 Converters for three-phase AC to DC and WECS

It has been identified in many works of literature that the presence of front-end DBR is siphoning off the precious energy generated from WECS [67]. Many solutions have been put forth, from using DAB to active bridge-based solutions [68]. A bridgeless converter has been used mostly for converting single-phase AC to DC in literature. Thus a new

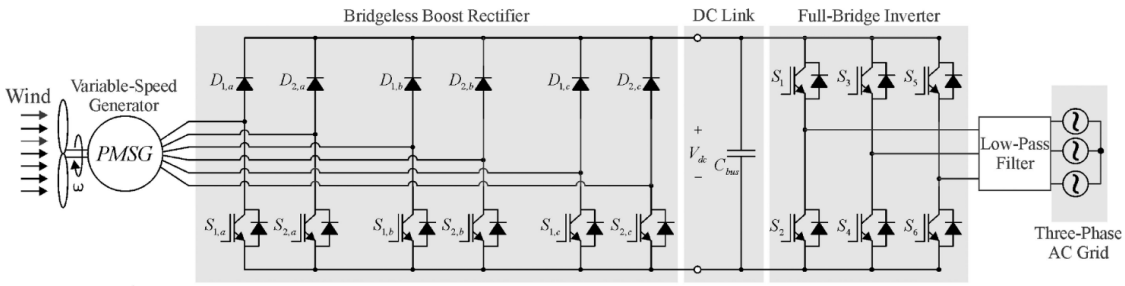

Figure 1.13: Proposed converter in [8] for WECS.

converter topology dealing with three-phase AC to DC conversion using bridgeless AC to DC converter has been presented. A single-phase bridgeless AC-DC converter with three-port output has been reported in [69].

The currently available bridgeless AC-DC converters are mostly designed for single-phase conversion systems. These converters increase the efficiency of the converter by eliminating the front end DBR [70–77] but are lacking in system performance, which can be achieved using three-phase systems. Three-phase power generation using PMSG or SEIG in a standalone system has a lesser cost and higher efficiency than a single-phase power generator [78, 79]. Maximum Power Point Tracking(MPPT) techniques for WECS are widely used by sensing torque and turbine speed or by sensing the DC current and voltages obtained after rectification [15, 80–84]. In the proposed system, there is no intermediate DC link after the three-phase generator; thus, a new MPPT technique is implemented.

Bridgeless boost converters exhibit excellent PFC, efficiency, ease of control, and low cost. However, the lack of a wide range of voltage control makes them unsuitable for MPPT across the available range of wind power. This problem is alleviated by using a buck stage as used in [85,86], which leads to a decrease in system efficiency.

The power electronic converters are the most vulnerable part of the WECS [87]; thus, a robust, efficient, and inexpensive AC to DC converter is needed [88,89]. In most of the PMSG fed conventional WECS, a front-end diode bridge rectifier (DBR) is used for rectification, followed by a DC-DC converter for power control and maximum power point tracking (MPPT) [80,90–93]. The decrease in efficiency due to front-end DBR and the popularity of bridgeless topology has recently motivated researchers to work toward a more efficient converter design for WECS.

A bridgeless boost rectifier is proposed in [8] for WECS, which requires connections

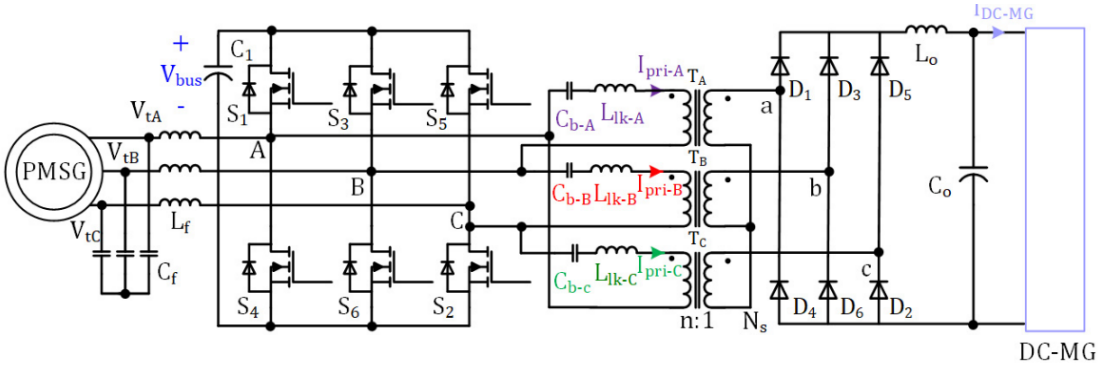

Figure 1.14: Topology of converter presented in [9] for WECS.

from all six terminals of PMSG and needs six switches for rectification, as shown in Figure 1.13. A compact AC to DC converter is proposed in [9], it has a higher number of switches, and an isolation transformer is used as well, thus increasing the cost and complexity of control shown in Figure 1.14.

A three-phase to DC converter is presented in [94] using space vector modulation, but it requires current sensors for power factor correction (PFC). All of these works need sensing of the generator voltage and current for controlling the power. A single-stage DC to three-phase AC converter is presented in [95], but cannot be used for WECS as it is unidirectional in nature thus cannot do AC to DC conversion. A bidirectional three-phase AC to DC converter is presented in [96]. It employs a boost strategy from both AC and DC sides and has three stages of conversion, resulting in increased component count and complexity. A unique three-phase AC to DC conversion strategy is proposed in [97] using coupled inductors, which needs two parallel converters and has high weight and cost due to the use of a large number of inductors. In this work, an efficient three-phase AC to DC converter is presented for power control of a wind turbine emulator-driven permanent magnet synchronous generator (PMSG). The details of converter working and operation with self-excited induction generator (SEIG) are given in [38].

1.6 Organization of the Thesis

This thesis deals with alleviating the limitations of PV and WECS. The problems in PV generations taken into account are the high voltage gain requirement of the converter to keep the string voltage at lower levels and the elimination of current ripple from the

output of the solar panels for removing the MPP oscillation. Furthermore, other aspects of a converter like the component reduction and reduction of voltage stress on the switches are explored as well. For WECS, the elimination of Front-end DBR and development of a unique MPP tracking(MPPT) technique, and the development of a wind turbine emulator are taken into account.

The thesis is organized as follows:

- Chapter 2 deals with the design and development of a low voltage-stress, high-gain converter using a coupled inductor. In this chapter, an interleaved topology of the converter is presented to reduce the input current ripple of the converter and reduce the current stress on the switching devices. As solar panels are low voltage high current sources inherently, the use of interleaved topology is preferred.

- Chapter 3 deals with the limitations of the converter developed in chapter 2 and thus presents a modified form of the converter with higher voltage gain. The interleaved topology of the converter is controlled in such a way that the current ripple is eliminated at all working duties. The only limitation of the converter is high voltage stress on the output side of the converter, and the input side switches experience reduced voltage stress compared to the conventional quadratic converter.

- Chapter 4 presents the three-phase AC to DC converter for WECS. This chapter presents a unique MPPT technique and explores the working of the converter with a SEIG driven by a wind turbine emulator. The wind turbine emulator is developed using a DC motor, following the characteristics of a MOD-2 wind turbine. The design technique and development requirements of the converter are stated in this chapter.

- Chapter 5 presents a topological change in the converter when fed from a PMSG. The stator inductance of the PMSG is used in place of the input side inductors in the converter, which enables the switching frequency of the converter to be as low as 10 kHz. The MPPT technique is changed as well from the input voltage, and current-based perturb and observe(P&O). The MPPT technique is changed to the TSR following. The wind turbine emulator is implemented using a SCIM with high power output.

- Chapter 6 deals with the development of HECS fed from solar and wind power generation systems. The comparison of the results obtained from the BESS controlled and single-phase grid controlled DC microgrid is presented in this chapter as well. The input-current ripple-free converter and the PMSG based WECS are combined to form the energy source of the HECS.

- The conclusion and future scopes of this work are presented in chapter 7 of this thesis.

After concluding this brief introduction of the PV generation system, WECS, and the HECS and presenting the literature review on the subject matter, the high gain converter with reduced voltage for solar/PV generation is presented in the next chapter.